KTH Industrial Engineering
and Management

Phase-field modeling of surface-energy driven processes

KLARA ASP GRÖNHAGEN

Doctoral Thesis
Stockholm, Sweden 2009

Materialvetenskap
KTH
SE-100 44 Stockholm
SWEDEN

ISRN KTH/MSE–09/39–SE+METO/AVH
ISBN 978-91-7415-426-9

Akademisk avhandling som med tillstånd av Kungl Tekniska högskolan framlägges till offentlig granskning för avläggande av teknologie doktorsexamen i materialvetenskap fredagen den 2 oktober 2009 klockan 10.00 i sal F3, Kungl Tekniska högskolan, Lindstedtvägen 26, Stockholm.

© Klara Asp Grönhagen, October 2009

Tryck: Universitetsservice US AB

Abstract

Surface energy plays a major role in many phenomena that are important in technological and industrial processes, for example in wetting, grain growth and sintering. In this thesis, such surface-energy driven processes are studied by means of the phase-field method. The phase-field method is often used to model mesoscale microstructural evolution in materials. It is a diffuse interface method, i.e., it considers the surface or phase boundary between two bulk phases to have a non-zero width with a gradual variaton in physical properties such as energy density, composition and crystalline structure.
Neck formation and coarsening are two important diffusion-controlled features in solid-state sintering and are studied using our multiphase phase-field method. Inclusion of Navier-stokes equation with surface-tension forces and convective phase-field equations into the model, enables simulation of reactive wetting and liquid-phase sintering. Analysis of a spreading liquid on a surface is investigated and is shown to follow the dynamics of a known hydrodynamic theory. Analysis of important capillary phenomena with wetting and motion of two particles connected by a liquid bridge are studied in view of important parameters such as contact angles and volume ratios between the liquid and solid particles.
The interaction between solute atoms and migrating grain boundaries affects the rate of recrystallization and grain growth. The phenomena is studied using a phase-field method with a concentration dependent double-well potential over the phase boundary. We will show that with a simple phase-field model it is possible to model the dynamics of grain-boundary segregation to a stationary boundary as well as a solute drag on a moving boundary.
Another important issue in phase-field modeling has been to develop an effective coupling of the Phase-field and CALPHAD methods. Such coupling makes use of CALPHAD's thermodynamic information with the Gibbs energy function in the phase-field method. With the appropiate thermodynamic and kinetic information from CALPHAD databases, the phase-field method can predict mictrostructural evolution in multicomponent multiphase alloys. A Phase-field model coupled with a TQ-interface available from Thermo-Calc is developed to study spinodal decompositon in FeCr, FeCrNi and TiC-ZrC alloys.

Keywords:Phase-field method, surface energy, solute drag, solid-state sintering, multicomponent multiphase flow, wetting, liquid-phase sintering, spinodal decomposition, CALPHAD

Preface

The research presented in this thesis was carried out at the division of Physical Metallurgy, Department of Materials Science and Engineering, the Royal Institute of Technology (KTH) in Stockholm, Sweden. In the first part, a short introduction to the field and some basic concepts are discussed. The second part consists of the following appended papers, that will be referred to in the text by their Roman numerals.

I. K. Asp and J. Ågren "Phase-field simulation of sintering and related phenomena - A vacancy diffusion approach"
Acta Materialia 54 (2006) 1241-1248

II. K. Grönhagen and J. Ågren "Grain-boundary segregation and dynamic solute drag theory - A phase-field approach"
Acta Materialia 55 (2007) 955-960

III. W. Villanueva, K. Grönhagen, G. Amberg and J. Ågren "Multicomponent and multiphase modeling and simulation of reactive wetting"
Physical Review E 77 (2008) 056313

IV. W. Villanueva, K. Grönhagen, G. Amberg and J. Ågren "Multicomponent and multiphase simulations of liquid phase sintering"
Submitted manuscript

V. K. Grönhagen and J. Ågren "Spinodal decomposition in FeCr and FeCr-based alloys; A phase-field approach coupled with CALPHAD database"
In manuscript

VI. K. Grönhagen, V.I. Razumovski, J. Odqvist, A.V. Ruban, P.A. Korzhavyi, M. Selleby and J. Ågren "Phase-field coupled with CALPHAD database and ab-initio modeling of diffusion barriers and prefactors for simulating spinodal decomposition in ZrC-TiC carbides"
In manuscript

Paper not included in this thesis:

K. Asp and J. Ågren "Phase-field simulation of sintering based on vacancy diffusion - effect on anisotropy"
TMS(The minerals, Metals and Materials society), 2005

Contents

Chapter 1

Introduction

The effect of surface energy is something we see everyday, for example water droplets and bubbles [1] or snowflakes with their complex and beautiful shapes. Surface energy can be viewed as the excess energy at the surface of a material compared to its inside (bulk). "Surface energy" (energy per unit area) is closely related to the surface stress or "surface tension" (force per unit length) and for liquids there is in fact no way to distinguish between surface energy and surface tension. The two terms are often used interchangeably. However, for solids the two quantities are generally different because surface energy is always a scalar quantity whereas surface tension is a tensor.
Surface energy is the basis for many industrial processes. It plays a major role in powder metallurgy, i.e., in the sintering process [2]. During sintering a powder mixture is turned into a solid body by bonding together the powder particles at high temperature. The micro-structural events occurring during sintering are driven by the lowering of excess energy attributed to surfaces and the pressure that develops under a curved surface. One may divide sintering into two different types; solid-state sintering, [3] and liquid-phase sintering [4], depending on whether or not any liquid phase is present. Many other processes of technological importance are also governed by the same physics, e.g. wetting [5], grain-boundary grooving [6, 7], grain growth etc.
Surface-energy driven processes are in general dynamic, i.e., the surfaces or interfacial boundaries evolve in time. Moreover, they are also so called free-boundary problems, i.e., the position of the moving boundary is not known a priori [8]. Mathematically, this is an interesting research topic and several methods for free-boundary problems exist. The treatment of a free boundary can be divided into two groups, sharp-interface methods and diffuse-interface methods. The front-tracking method is a sharp-interface method and it explicitly tracks the moving interface by "markers". The markers are evenly distributed on the phase boundary. The level-set method could also be viewed as a sharp-interface method although the implementation is diffuse. In level-set

methods the problem of explicit front tracking is avoided by introducing an extra field variable Φ, which is called level-set function. For every point in the domain, the level-set function gives the distance to the zero level-set (defined as the middle of the interface). In both Front-tracking and Level-set methods the governing equations are solved on an underlying grid, which is kept fixed. Hence, the grid does not in general match the interfaces, which are separately represented. Different free-boundary problems, for example incompressible two-phase flow and solidification (Stefan problem) have been modeled by front-tracking methods [9, 10] and level-set methods [11, 12], respectively.
The phase-field method is a diffuse-interface method to model free-boundary problems. It considers the phase interface to have a non-zero width with a gradual variation in physical properties such as energy density, composition and crystalline structure. The position of the interface, and the state of the system is given by the variation in so called phase-field variable(s). In the simplest case of a phase transformation the phase-field variable has constant but different values in the two bulk phases and varies smoothly over the interface. The phase-field method is able to predict the evolution of arbitrary phase boundaries without explicitly tracking the position of the interfaces. Examples of phase-field methods used to model incompressible two-phase flow can be found in [13] and solidification in [14, 15].

1.1 Overview and aim of thesis

In the present thesis, we investigate typical surface-energy driven processes of technological importance by means of the phase-field method. The aim is to enable new and better methods for microstructure design as well as the design of processing alloys with unique properties. One important material process is sintering. A multiphase phase-field method with diffusion as material transport mechanism is developed in Paper I to model solid-state sintering. Neck formation and coarsening of a two-particle system is investigated as well as grain-boundary grooving. An analysis of dihedral angles by means of interfacial energies is presented.
A multicomponent multiphase phase-field method, built on the same concept (as in Paper I) but also including fluid flow by Navier-stokes equation with surface tension forces and convective phase-field equations are presented in Paper III and IV. This model can predict reactive wetting and rigid-body motion, typical features in liquid-phase sintering.
The rate of coarsening or grain growth can be affected by the interaction between solute atoms and migrating grain boundaries. This is known as solute drag and the phenomena has been studied at KTH for many years. In Paper II, we present a phase-field method with a concentration dependent double-well potential over the phase boundary to take solute drag into account.
In order to make it possible to model microstructure evolution of real alloys, especially complex multicomponent alloys, coupling of phase-field and CALPHAD

methods is necessary. Such coupling makes use of CALPHAD's thermodynamic information with the Gibbs-energy function in the phase-field method. A phase-field model using CALPHAD method is presented in Paper V to study spinodal decomposition in FeCr and FeCr-based alloys and in Paper VI to study spinodal decomposition in TiC-ZrC alloys. In Paper VI, due to inadequate kinetic information, ab-initio calculations were performed to give diffusion barriers and pre-exponential factors in the ZrC-TiC system.
The main results are given in the second part of this thesis (the appended papers). The first part is intended to give an overview of the topic and is organized as follows. Chapter 2 contains the basics of the phase-field method. In Chapter 3 we discuss wetting and sintering and the phase-field models used. Chapter 4 describes solute drag and phase-field modeling of solute drag. Chapter 5 describes phase-field modeling of spinodal decomposition and in Chapter 6 we discuss phase-field coupling to CALPHAD databases and some numerical aspects. Finally, we summarize the appended papers, present our conclusions and discuss future prospects in Chapter 7.

Chapter 2

Phase-field methods

The phase-field method is often used to model microstructural evolution in materials. The method is generally known to originate from Cahn and Hilliard's [16] work on free energy of a nonuniform system and Allen and Cahn's work [17] on antiphase boundary motion. Based on their work, several phase-field methods have been developed to model solidification [19], [20], grain growth [21], [22] and wetting [23], [24] to name a few. For a general review on phase-field methods see for example [25]. It should be mentioned though that the diffuse-interface concept was introduced already in the late 19:th century by van der Waals [26] in his analysis of the capillarity effect in critical systems.
Phase-field models are based on the total value of a suitable thermodynamic state function, i.e., it is given by a functional. For a thermodynamically consistent derivation of a isobarothermal binary system the functional will be the total Gibbs energy of the system and may be expressed as

$$G = \int_{\Omega} \left(f(u,\phi) + \epsilon_u^2 |\nabla u|^2 + \epsilon_\phi^2 |\nabla \phi|^2 \right) d\Omega \tag{2.1}$$

where f is the Gibbs energy density, i.e. G_m/V_m, G_m and V_m being the molar Gibbs energy and volume, respectively. The molar Gibbs energy is described by a double well potential, u is a variable representing the composition, i.e. the u-fraction and ϕ is the phase-field variable taking the value 0 in one phase and unity in the other. Ω is the domain of the system. The parameters ϵ_u and ϵ_ϕ are gradient coefficients. The u-fraction represents a conserved quantity and time evolution is governed by the normal conservation law,

$$\frac{\partial u}{\partial t} = -\nabla \cdot J \tag{2.2}$$

To obtain an expression for the diffusional flux J, Onsager linear law of irreversible thermodynamics is applied,

$$J = -L'' \nabla \frac{\delta G}{\delta u} \tag{2.3}$$

The phase-field variable is a non-conservative quantity and the following type of linear equation is often used,

$$\frac{\partial \phi}{\partial t} = -M_\phi \frac{\delta G}{\delta \phi} \tag{2.4}$$

where M_ϕ is a kinetic quantity related to the interfacial mobility. Equation 2.4 is usually referred to as the Allen-Cahn equation or the time-dependent Ginzburg-Landau equation. The combination of eqs. 2.2 and 2.3 leads to the well-known Cahn-Hilliard equation.

$$\frac{\partial u}{\partial t} = \nabla L'' \nabla \frac{\delta G}{\delta u} \tag{2.5}$$

The solution of Eqs. 2.4 and 2.5 yields the microstructural evolution of the system.
As can be seen both equations are expressed in terms of the variational derivatives of the the functional G. In problems involving phase change as well as diffusion both type of equations are used, see for example [27] for formation of Widmanstätten plates in the Fe-C system. In cases where there is no change in crystalline structure only the Cahn-Hilliard equation is used, e.g. in spinodal decomposition, see [28] and in the case there is only change in crystalline structure and no diffusion, e.g. martensitic transformation, only Allen-Cahn equation is used, see for example [44]. Once the appropriate equations have been chosen in accordance with the problem of interest one has to choose the form of the Gibbs energy curve, i.e. how does the Gibbs energy vary with the phase-field variable. If the Gibbs energy curve has two minima and describes a double-well potential, the Cahn-Hilliard equation is applicable and the variable ϕ can be neglected. Thus, only Eq. 2.5 will be solved. On the other hand, if the system is described by several Gibbs energy curves, one for each phase, the curves have to be connected to create a double well potential and this is achieved by including the phase-field variable ϕ meaning that both Eqs. 2.5 and 2.4 need to be solved. Sometimes one distinguishes between the Cahn-Hilliard model when only Cahn-Hilliard equations are solved and the Allen-Cahn model when the Allen-Cahn equation is solved simultanously with a normal diffusion equation, i.e. neglecting the composition gradient term.

Surface energy

Surface energy can be viewed as the excess energy at a surface, grain boundary or phase boundary of a material compared to the inside (bulk). These interfacial regions have always a higher energy than the bulk, i.e. the surface energy can never be negative. Otherwise there would be a driving force to create phase

boundaries everywhere. In phase-field methods the surface energy is defined as the difference per unit area of the interface between the actual Gibbs energy $G_m(u,\phi)$ and the Gibbs energy of the system if all properties were homogeneous in each phase and the interface was sharp [16] .

$$\sigma = \int_0^{\delta} \Big(\frac{\Delta G_m(u,\phi)}{V_m} + \epsilon_u^2 |\nabla u|^2 + \epsilon_\phi^2 |\nabla \phi|^2 \Big) dg \tag{2.6}$$

where g is the distance across the interface in its normal direction. $\Delta G_m(u,\phi)$ is the difference between $G_m(u,\phi)$ and the bulk Gibbs energy. δ is the thickness of the interface.

2.1 Cahn-Hilliard model

The total Gibbs energy in a binary system of elements A and B is based on the functional G (Eq. 2.1 but without the variable ϕ)

$$G = \frac{1}{V_m} \int_\Omega \left(G_m(u_A) + \epsilon^2 |\nabla u_A|^2 \right) d\Omega \tag{2.7}$$

G_m denotes the molar Gibbs energy as available from CALPHAD-type of databases, V_m the molar volume that will be approximated as constant. The parameter ϵ is the gradient energy coefficient. u_A is the u-fraction of the A atoms. The evolution of the concentration field is governed by the normal conservation equation,

$$\frac{1}{V_m} \frac{\partial u_A}{\partial t} = -\nabla \cdot J_A \tag{2.8}$$

We have assumed that the diffusional flux of solutes J_A is given by the Onsager linear law of irreversible thermodynamics and adopt the following form if A is a substitutional element.

$$J_A = -L'' \nabla \left(\frac{\delta G}{\delta u_A} \right) = -\frac{L''}{V_m} \nabla \left(\mu_A - \mu_B \right) \tag{2.9}$$

where B denotes the other element. Including the gradient energy, the chemical potential difference, sometimes called the diffusion potential, is given by

$$\mu_A - \mu_B = \frac{\partial G}{\partial u_A} - \frac{\partial G}{\partial u_B} - 2\epsilon^2 \nabla^2 u_A \tag{2.10}$$

L'' denote the phenomenological coefficient and is related to the atomic mobilities M_A and M_B of the elements A and B respectively, as,

$$L'' = u_A(1-u_A)((1-u_A)M_A + u_A M_B) \tag{2.11}$$

The resulting independent diffusion equation for A becomes (the equation for B is dependent),

$$\frac{du_A}{dt} = \nabla\Big(L''\nabla\Big(\frac{\partial G}{\partial u_A} - \frac{\partial G}{\partial u_B} - 2\epsilon^2\nabla^2 u_A\Big)\Big) \tag{2.12}$$

Equation 2.12 is the Cahn-Hilliard equation for $A-B$ binary system.

2.2 Allen-Cahn model

Here, we present a commonly used phase-field approach following the work by Warren and Boettinger [20]. The total Gibbs energy in a binary system of elements A and B is based on the functional G (Eq. 2.1),

$$G = \int_\Omega \left(\frac{G_m(u_A,\phi)}{V_m} + \epsilon_\phi^2|\nabla\phi|^2\right) d\Omega \tag{2.13}$$

but the gradient coefficient of composition is neglected ($\epsilon_u^2 = 0$). $G_m(u_A,\phi)$ is the molar Gibbs energy and is postulated as a function of u_A and ϕ,

$$G_m = (1-P(\phi))G_m^\alpha + P(\phi)G_m^\beta + g(\phi)W \tag{2.14}$$

where G_m^α and G_m^β denote the molar Gibbs energy as available from CALPHAD-type of databases, for the α and β phase, respectively. $P(\phi)$ is an interpolating function which takes the value $P(0)=0$ and $P(1)=1$. $g(\phi)W$ is a term that determines the height of the double-well potential over the phase interface.
The evolution of the phase-field variable is governed by the Allen-Cahn equation (Eq. 2.4),

$$\frac{\partial\phi}{\partial t} = -M_\phi\Big(\frac{1}{V_m}\frac{\partial G}{\partial\phi} - 2\epsilon^2\nabla^2\phi\Big) \tag{2.15}$$

Combining Eq. 2.3 and Eq. 2.2 we get the following diffusion equation,

$$\frac{\partial u_A}{\partial t} = \nabla\Big(L''\Big(\frac{\partial^2 G_m}{\partial u_A^2}\nabla u_A + \frac{\partial^2 G_m}{\partial u_A\partial\phi}\nabla\phi\Big)\Big) \tag{2.16}$$

Equations 2.15 and 2.16 are the two basic equations to be solved in the binary Allen-Cahn system. It should be emphasized that Eq. 2.16 does not contain any gradient energy term. The factor $\partial^2 G_m/\partial u_A^2$ corresponds to the well known Darken's thermodynamic factor.

Chapter 3

Wetting and Sintering

Wetting and sintering are very important surface-energy driven processes [29]. Sintering may be regarded as the basis of powder metallurgy. Wetting is important in the bonding or adherence of two materials and therefore important for the sinterability of a powder system.

3.1 Wetting

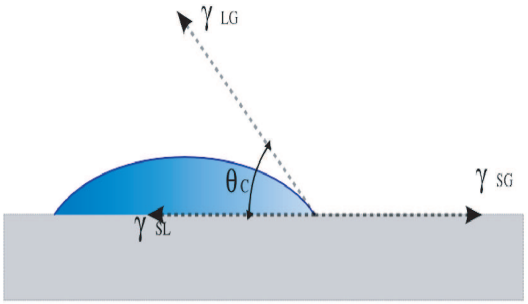

Figure 3.1: Interfacial energies and contact angle. After reference [32]

Wetting is the ability of a liquid to maintain contact with a solid surface [30]. In total wetting the fluid spreads completely over the surface. On the contrary, in partial wetting, the fluid will rest on the solid surface with a finite contact angle θ_c. Good wetting is characterized by a small contact angle and bad wetting, on the other hand, is characterized by a large contact angle. The wettability for a fluid on a flat rigid surface depends on the surface tension forces giving rise to a contact angle θ_c determined by Young's law [31].

$$cos\theta_c = \frac{\gamma_{SG} - \gamma_{SL}}{\gamma_{LG}} \tag{3.1}$$

where the respective phase boundaries are solid-gas, SG, solid-liquid, SL and liquid-gas, LG. Figure on wetting on a solid rigid surface, see Fig. 3.1. An early work on phase-field modeling of wetting, see [23] and more recently [24].

Reactive wetting

In reactive wetting the solid surface is not inert [4], see fig. 3.2. Chemical change and/or diffusion of material is taking place between the liquid and the solid. Thus, solubility. i.e how much material that can be dissolved in the liquid/solid is an important thermodynamic parameter.

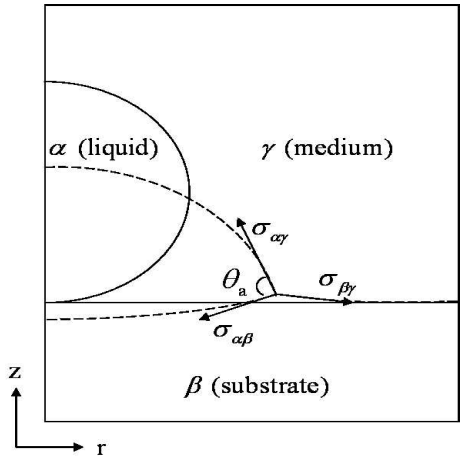

Figure 3.2: Reactive wetting with depletion of the liquid(α) into the solid (β). After figure in Paper III

In Paper III, we present a multicomponent multiphase phase-field model with fluid motion and is utilized to simulate reactive wetting. The model is based on the concepts of multiphase phase-field modeling developed in Paper I together with Villaneuva and Amberg's work on capillary-driven flows [24]. The basic concept is to include convection into the Allen-Cahn model and then treat solid phases as phases that have a very high viscosity. Thus, convective flow is suppressed in the solid phases and the only material transport allowed there is diffusion. On the contrary, the liquid phase allows for both diffusion and convection as material transport mechanisms.

To account for convection, the Navier-Stokes equation with surface-tension forces is introduced,

$$\rho \frac{Dv}{Dt} = -\nabla p + \mu \nabla^2 v - \phi \nabla \frac{\delta G}{\delta \phi} \tag{3.2}$$

which is combined with the condition of incompressible flow,

$$\nabla \cdot v = 0 \tag{3.3}$$

Here v is the velocity, ρ is the density, p is the pressure, μ is the viscosity. The last term in Eq. 3.2 describes the surface-tension forces. This term has to be included when coupling Navier-Stokes equation with the Allen-Cahn equations. The expression follows the same derivation for surface-tension forces when coupling Navier-Stokes equation with Cahn-Hilliard equation [13]. D stands for the material derivative ($\frac{Dv}{Dt} = \frac{\partial v}{\partial t} - v \cdot \nabla v$) and it describes the transport of a vector quantity (or scalar) in a velocity field, which is known as convection. Further, since there is now also convection taken into account, the time derivatives in the Allen-Cahn equations (Eqs. 2.15 and 2.16) have to be changed into material derivatives.
Analysis of a spreading liquid on a non-inert surface is investigated. Two stages of wetting are revealed. First, the convection-dominated stage where fast spreading occurs. Second, the diffusion-dominated stage where chemical change between the liquid and surface occurs. Experimental studies on reactive wetting also report two stages of a spreading liquid [33, 34]. For a detailed description and analysis of the dynamics see Paper III.

3.2 Sintering

Materials or objects that are difficult to produce with conventional casting may be produced by compacting a powder and sinter it to a solid body. Cemented carbides, sinter steel and ceramics are technologically important examples. Sintering is the bonding together of particles at high temperature. In solid-state sintering the material is heated to a temperature below its melting point. On the other hand, if the temperature is high enough for some liquid phase to form it is called liquid-phase sintering. The decrease in total surface energy yields the driving force for various diffusion processes and convection that usually lead to a lowering of porosity and a densification of the material.

Solid-state sintering

During solid-state sintering a powder compact is gradually transformed into a solid body. The structural changes associated with solid-state sintering depend on

different diffusion processes. For metal powders, the diffusion processes are surface diffusion, diffusion along the grain boundaries or diffusion through the crystalline lattice [61, 36]. Important parameters in solid-state sintering are for example the size distribution of the particles; the size of the sintering particles affects the sintering time because the surface energy per unit volume depends on the inverse of the particle diameter. Thus, smaller particles with high specific surface area have more energy and sinter faster. The first step in solid-state sintering is the neck formation between particles. At each particle contact, a grain boundary grows to replace the vapor-solid interface. The dihedral angle (fig. 3.3), i.e., the angle between the connected particles close to the grain boundary is determined by the grain-boundary energy and the energy of the particle-vapor surface by means of

$$2cos(\phi/2) = \sigma_{SS}/\sigma_{SM} \tag{3.4}$$

where σ_{SS} is the grain boundary energy and ϕ the dihedral angle. The later stage in solid-state sintering is migration of grain boundaries so that smaller particles merges into larger particles, so called coarsening or Ostwald ripening.

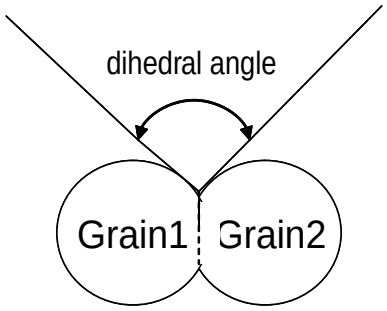

Figure 3.3: Dihedral angle. After figure in Paper I

In paper I we discuss a multiphase phase-field model for simulating neck formation and coarsening of a two-particle system. Analysis of the dihedral angle by means of the interfacial energies are investigated as well as grain-boundary grooving on an initial T-shaped triple junction.

Liquid-phase sintering

During liquid-phase sintering one of the powder components melts during the sintering process, [4] for example cobolt (Co) when producing cemented carbides [58, 59]. For complete densification by liquid-phase sintering several parameters are important, such as the amount of liquid, solubility of the solid in the liquid

and wetting between the liquid and the solid particles. The densification process in liquid-phase sintering can usually be divided into three steps, namely; rearrangement, solution-reprecipitation and solid-state sintering. In the rearrangement step, the liquid spreads and wets the solids resulting in capillary forces and rearrangement of particles and denser packing. In the second stage, densification occurs by diffusion of atoms by solution-reprecipitation of solids. Material is dissolved from solid-liquid interfaces with high chemical potential, i.e small particles and reprecipitated on interfaces with lower chemical potential, i.e., large particles, leading to coarsening. The later stage is a slow densification process, described by typically solid-state sintering processes.

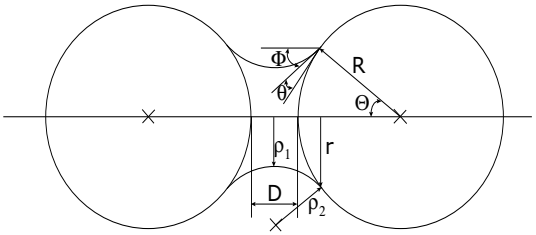

Figure 3.4: Geometry of two particles connected by a liquid bridge. After reference [60]

Liquid-phase sintering, including both diffusion and convection is discussed in paper IV and is based on the model developed in paper III. Important dynamics in liquid-phase sintering such as rapid wetting and motion of particles due to capillarity is studied. Parameters affecting the dynamics are interfacial energies and the volume ratio between liquid and solid particles. Analysis of an idealized two-particle system connected by a liquid bridge is investigated by means of contact angles and volume ratios and compared with an analytical model by Huppman and Riegger [60]. Figure 3.4 shows a schematic of the two-particle system studied. The comparison showed good agreement between phase-field simulations and the analytical model giving support to both approaches.

Chapter 4

Solute drag

Grain growth is a surface-energy driven process. Grain growth occurs by migration of grain boundaries where small grains are consumed by larger grains leading to an increase in average grain size (Coarsening). It is well known that interaction between solute atoms and migrating grain boundaries may have a pronounced effect on the rate of grain growth and recrystallization. The effect was first observed a long time ago by Beck [37] who reported that the time for recrystallization of lead could be increased by many orders of magnitude by adding ppm levels of Ag. However, he did not offer any explanation for this behavior. Much later this phenomenon was found to stem from segregation of solute atoms to the grain boundary and their drag effect on a migrating grain boundary, so called solute drag. The first theoretical analysis was presented by Lücke and Detert [38] but the first satisfactory theoretical treatment was presented by Cahn [39] and was based on a steady-state solution of the diffusion equation across the moving grain boundary. For a stationary boundary the concentration profile is symmetric and given by the thermodynamic equilibrium but as the boundary moves the profile becomes asymmetric and there will be a retarding force, a drag force, see Fig 4.1. Cahn obtained the drag force by integration over the concentration profile,

$$P_i = -N_v \int_{-\infty}^{\infty} (C(x) - C_0(x)) \frac{dE}{dx} dx \tag{4.1}$$

$C(x)$ is the concentration of solutes over the grain boundary and $C_0(x)$ is the concentration of solutes far from the grain boundary. The interaction energy is denoted E and is assumed to have a triangular shape over the boundary. The concentration profile has to be known prior to the integration. Later Hillert and Sundman [45] like Cahn took the concentration profile from the steady-state solution but considered the Gibbs-energy dissipation rather than the drag force. Like the drag force the dissipation is obtained by integration. Hillert and Sundman also showed that their treatment is equivalent with Cahn's treatment

for grain-boundary migration but has the advantage that it can be applied to phase transformations without any extra difficulty. The dissipation model by Hillert and Sundman has been developed further by Odqvist et al [46, 47], and later Hillert presented a new formulation of Cahn's solute drag equation which makes the solute drag and the dissipation approach equivalent also for phase transformations [48]. For phase-field modeling of solute drag, see [49, 50, 51].

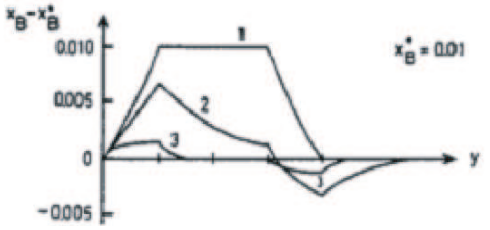

Figure 4.1: Schematic of the concentration profile over the grain boundary at different migration rates. 1,2,3 increasing velocity. After reference [45]

In the appended paper II, we show that is it possible to model the dynamics of grain-boundary segregation to a stationary boundary as well as solute drag on a moving boundary with the same phase-field approach. It is achieved by introducing a concentration dependency in the height of the double-well potential in the Gibbs energy expression (Eq. 2.14),

$$W(u_A) = W_B(1 - u_A) + W_A u_A \tag{4.2}$$

where W_A and W_B are two coefficients to be determined from experimental data on grain-boundary energy and grain-boundary segregation. u_A is the u-fraction of solutes. Analysis of grain-boundary segregation is investigated and compared to McLean's analytical solution [40] and moreover, dynamic solute drag with a build up of a concentration spike on a moving boundary and the resulting retarding force are simulated, as well as the disappearence of the concentration spike for high driving forces. For further details, see Paper II.

Chapter 5

Spinodal Decomposition

Phase separation in a solid solution is a mechanism where a homogeneous solution separates into distinct regions with different alloy compositions. This happens if the mean composition is inside a misciblility gap of the phase diagram. Within a miscibility gap two different domains exist, reflecting how the phase separation arises, namely outside the spinodal line where the phase separation occurs by nucleation and growth and inside the spinodal regime where the phase separation occurs throughout the parent phase, the so called spinodal decomposition. Figure 5.1 shows a schematic phase diagram containing miscibility gap. The spinodal line is defined as the locus of points where the second derivative of Gibbs energy vs. composition is zero. Inside the spinodal regime the thermodynamic factor in the diffusion coefficient thus becomes negative and consequently the diffusion coefficient also becomes negative. The first theoretical treatment of spinodal decomposition was presented by Hillert [18] who considered diffusion in a binary alloy by means of a 1-dimensional discrete-lattice model and nearest neighbor interactions. For an inhomogeneous system he found an extra contribution to the free energy proportional to the squared difference in content between two neighboring lattice planes. Cahn and Hilliard [16] rather considered a continuous variation in composition and properties and added an extra term proportional to the concentration gradient squared. They called the extra term the gradient energy. Later Cahn [28], inspired by Hillert's work, combined the continuum approach and a diffusion equation. The inclusion of the gradient energy gave a modified diffusion equation which is now called the Cahn-Hilliard equation. For phase-field modeling of spinodal decomposition in Fe-Cr-Co [41], Fe-Cr-Mo [42] and [43] for a general ternary Cahn-Hilliard model with degenerate mobility.

5.1 Spinodal decomposition in ferrite

Duplex stainless steels have a two-phase structure containing austenite and ferrite [52]. The traditional applications of duplex stainless steels can be found in the

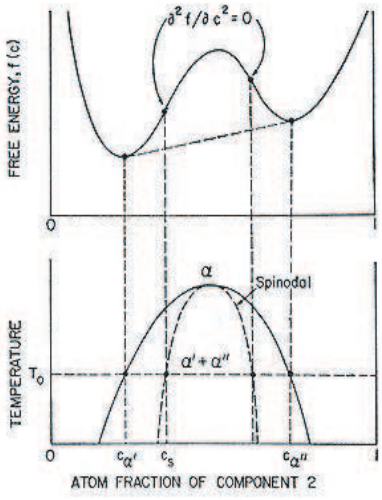

Figure 5.1: Schematic of the double-well free energy curve (above) and phase diagram showing the miscibility gap (below). After reference [54].

chemical, oil and gas industries. The two-phase structure combines the beneficial effects of the two different phases, namely high strength (ferrite) and toughness (austenite) even at low temperatures. However, at high temperatures (above 250^oC), the ferrite phase loses impact toughness and becomes brittle. This behavior is known as 475^oC embrittlement. The embrittlement is due to phase separation where the ferrite phase(α) decomposes into an Fe-rich α-phase and a Cr-rich α'-phase. This phase separation occurs because there is a miscibility gap below 500^oC in the FeCr phase diagram. The existence of a miscibility gap in FeCr system was first suggested by Williams and Paxton [53] and later confirmed by Chandra and Schwartz [55].
In paper V, we present a phase-field model of spinodal decomposition in FeCr and FeCrNi systems. All thermodynamic and kinetic information is imported from available thermodynamic databases, see Chapter 6.2 for further details on coupling phase-field and CALPHAD methods. The simulated results are compared to experimental studies on binary FeCr-system [56] and ternary FeCrNi system [57].

5.2 Spinodal decomposition in carbides

Hard metals, or cemented carbides are widely used as cutting tools because of their high strength. In many applications they have replaced convential high speed steels. Cemented carbides is a class of composite materials, consisting of a

mixture of carbides, which provides hardness and wear resistance and metal binder providing toughness [58]. The carbides are usually metal carbides, mostly tungsten carbides (WC) and for example ZrC, TiC, NbC and TaC. The metal binder is almost exclusively Cobolt (Co). One interesting metal carbide system used when producing cemented carbides is the ZrC-TiC system. It is an interesting system because it has a miscibility gap, meaning that phase separation will occur in the carbide. This may have a beneficial effect on the cemented carbide since in general phase separation will make a material harder. Early experimental studies on the miscibility gap in the ZrC-TiC system have been carried out by Kieffer et al [62] and more recently by Markström et al [63]. In Paper VI a phase-field model coupled with CALPHAD database and using ab-initio calculations for the diffusion barriers and pre-exponential terms is developed to simulate spinodal decomposition in a ZrC-TiC carbide system.

Chapter 6

Simulation software

6.1 FemLego

Through out this work, all simulations were carried out using the symbolic computational tool FemLego [64, 65]. It consists of a set of Maple procedures and Fortran routines. It can be used to solve partial differential equations with adaptive finite element method.
The standard procedure for setting up the variational form is to multiply the partial differential equation with a test function and integrate over the entire domain, applying integration by parts and choosing appropriate base functions. The phase-field equations as well as Navier-Stokes equation are discretized in space using piecewise linear functions. The resulting linear systems are then solved using appropriate solver. Notice, the Navier-Stokes equation is solved using a projection method by Guermond and Quartapelle [66] with an added pressure stabilization term. The use of adaptively is essential since the phase-field methods requires the interface to be resolved with at least 5 grid points. An Ad hoc error criterion is used to ensure mesh resolution on the phase boundary.

6.2 Thermo-Calc and DICTRA used in simulations

An important issue in the present work has been to couple Phase-field and CALPHAD methods. Such coupling makes it possible model microstructure evolution of complex multicomponent alloys. The CALPHAD technique [69] is very useful for obtaining thermodynamic equilibrium information. The equilibrium state at a given composition, temperature and pressure can be calculated by minimizing the total Gibbs energy of all phases in the system. An advanced software using the CALPHAD technique is Thermo-Calc software [68, 67]. In addition, DICTRA is a software package [71, 72] that solves multicomponent diffusion equations in multiphase regions and is coupled to Thermo-Calc and kinetic databases.

The idea with coupling phase-field and Thermo-Calc is to use CALPHAD's thermodynamic information with the Gibbs energy function in the phase-field method. To retrieve thermodynamic and kinetic information, Thermo-Calc has different programming interfaces to enable interaction with the Thermo-Calc kernel and programming languages. In Paper V and VI, a Fortran based TQ-interface [?] is used to make Thermo-Calc an integral part of FemLego. For a general discussion on coupling Phase-field and CALPHAD methods, see [73] or MICRESS [74] for a software package coupling multiphase-field concepts with Thermo-Calc.

Chapter 7

Concluding remarks

7.1 Summary of the appended papers

Paper I

Phase-field simulation of sintering and related phenomena - A vacancy diffusion approach

We have developed a multiphase phase-field model. The governing equations are the multiphase Allen-Cahn equations with diffusion equations to represent material transport mechanisms. Each grain or phase is represented by a phase-field variable with the constraint that all phase-field variables must sum up to 1. Input parameters are interfacial energies and an idealized phase diagram. The model is used to simulate neck formation and coarsening of a two-particle system. Analysis of the dihedral angle by means of the interfacial energies is performed as well as grain boundary grooving on an initial T-shaped triple junction.
The respondent did all the work with input from J. Å.

Paper II

Grain-boundary segregation and dynamic solute drag theory - A phase-field approach

We present a phase-field model to study grain-boundary segregation and solute drag in a binary alloy. The governing equations are the Allen-Cahn equations with a concentration dependency in the height of the double-well potential in the Gibbs energy expression. We show that the model is capable to simulate the dynamics of grain-boundary segregation to a stationary boundary as well as solute drag on a moving boundary. Analysis of grain-boundary segregation is investigated and compared with McLean's analytical solution [40] and moreover, the dynamics of

solute drag on a moving grain-boundary, including the build-up of a concentration spike in the boundary and the resulting retarding force are investigated, as well as the disapearence of the concentration spike at high velocities.
The respondent did all the work with input from J. Å.

Paper III

Multicomponent and multiphase modeling and simulation of reactive wetting

We present a multicomponent multiphase phase-field model with fluid motion. The model is used to simulate reactive wetting. The governing equations are convective phase-field equations coupled with Navier-Stokes equation with surface tension forces. Idealized phase-diagram, surface energies and some typical dimensionless numbers are input parameters into the model. An axisymmetric model with adaptive finite element method are utilized. Very high viscosity is implemented into the solid phase in order to suppress any convection there. Typical ratio of the viscosity between liquid/solid is 10^5. Analysis of a spreading liquid on a surface is investigated. Two stages of wetting are revealed. First, the convection-dominated stage where fast spreading occurs. Second, the diffusion-dominated stage where chemical change between the liquid and surface occurs. The dynamics of the first stage is shown to match a hydrodynamic theory by Cox for spreading liquids [35]. The diffusion dominated stage are determined by solubility of the liquid/solid phases, surface energies and mobilities.
The model was based on previous work of all authors. The respondent implemented the model together with W.V. with feedback from J.Å. and G.A. and contributed to the discussion of the results.

Paper IV

Multicomponent and multiphase simulations of liquid phase sintering

Using the model developed in Paper III, numerical simulations of liquid-phase sintering are presented. Important dynamics in liquid-phase sintering such as rapid wetting and motion of particles due to capillarity is studied. Parameters effecting the dynamics are interfacial energies and volume ratios between liquid and solid particles. The two-particle system connected by a liquid bridge is investigated by means of interfacial energies and volume ratios and compared with an analytical model by Huppman and Riegger [60]. The comparison showed good agreement between the phase-field simulations and the analytical model.
The model used is similar to Paper III. The respondent did the analytical comparison, wrote parts of the paper and contributed to the discussion of the results.

Paper V

Spinodal decomposition in FeCr and FeCr-based alloys; A phase-field approach coupled with CALPHAD database

In this paper, we present a coupling of phase-field and CALPHAD methods to simulate spinodal decomposition in FeCr and FeCrNi systems. The governing equations are the binary and ternary Cahn-Hilliard equations with thermodynamic and kinetic information from Thermo-Calc. A Fortran based TQ-interface is used to make Thermo-Calc an integral part of FemLego. To speed up the simulation time, all thermodynamic and kinetic data are stored in a matrix with linear interpolations performed between the values. The simulated results show a good agreement in morphology and kinetics compared with experimental studies [56, 57] in the binary system, whereas for the ternary system, the model did not predict the kinetics very well. In addition, simulations on a binary Fe-Cr alloy close to the spinodal line were carried out. The change from nucleation and growth to spinodal decomposition may not be a sharp limit. Simulated results show that the classical nucleation and growth theory may not be valid close to the spinodal line. These results are in agreement Hillert's [18] analysis on critical wave length and fluctuations in the miscibility gap.
The respondent did all the work with input from J. Å.

Paper VI

Phase-field coupled with CALPHAD database and ab initio modeling of diffusion barriers and prefactors for simulating spinodal decomposition in Zr-C-TiC carbides

The model used is similar to Paper V, but in the present paper we perform numerical simulations on a ZrC-TiC system. An experimental investigation and thermodynamic assessment of the miscibility gap were performed at unit carbon activity by Markström et al.[63]. We treat the system as a system with two sublattices (Ti,Zr)(C,Va) and solve for the u-fraction of Zr under the condition that the activity of Carbon is unity. Due to lack of information on mobilities of the present system in DICTRA and poor information in literature, ab initio calculations were performed to give values of diffusion barriers and pre-exponential factors for Zr diffusion in ZrC and Ti diffusion in TiC. The results show that spinodal decomposition is not controlled by bulk-diffusion of Metal atoms. One suggestion is that liquid Co acts as a transport medium of Zr,Ti and C.
The respondent did all the phase-field simulations with input from J.O. and J.Å. and was the principal author.

7.2 Conclusions and future prospects

The aim of this work was to create new and improved methods for design of microstructures and processing of alloys. Focus has been on surface-energy driven processes of technological importance by means of the phase-field method. We have developed new methods to simulate important features in solid-state and liquid-state sintering. Dihedral angles, contact angles, wetting, reactive wetting, coarsening and motion of particles are phenomena which have been successfully studied. A new phase-field model to simulate solute drag has also been developed, important in grain growth and recrystallization. Finally we have coupled Phase-field and CALPHAD methods which enables the modeling of real microstructure evolution of complex multicomponent alloys. Such coupling is more or less necessary when modeling real microstructure evolution of complex multicomponent alloys.
One important achievement of our work is the ability to couple CALPHAD methods with all phase-fields methods developed within this thesis. In order to simulate for example liquid-phase sintering of cemented carbides, one would like to incorporate an appropriate phase-diagram of WC-Co-gas. Here, one demanding issue is how to treat the surrounding phase, usually a gas. In a real system, the solubility of Co and WC in gas is is exceedingly low but this limit is not numerically feasible given our current method.
Despite the fact that the binary Fe-Cr and Fe-Cr-based systems are important systems when developing different steel products, it is surprising how little experimental information there is at temperatures below 500^oC. This is of course a strong limitation when modeling phase separation in Fe-Cr and Fe-Cr based ternary systems. During our work on studying important features in 475^oC embrittlement we realize that we do not know how the nucleation and growth appears close to the spinodal line. Is it a gradual change from nucleation and growth to spinodal decomposition, a sharp limit or is the classical nucleation and growth theory not valid close to the spinodal line? And where is the spinodal line?
One important improvement of the ternary Cahn-Hilliard model is to investigate how much the gradient energy coefficients affect the kinetics. In order to handle negative interaction parameters, one suggestion is to include a non-conservative variable to account for ordering in the system. Multicomponent systems with miscibility gaps often contain some negative interaction parameters indicating a tendency for ordering. Such ordering should be included in the model, e.g. by introduction of a non-conservative order parameter. Nevertheless, this thesis has highlighted the usefulness of the phase-field method to model many important material processes.

Acknowledgments

The financial support from the Swedish Foundation for Strategic Research (SSF) and the VINNEX centre HERO-M, financed by VINNOVA, the Swedish Goverment agency for Innovation Systems and the Royal institute of Technology. A large number of people have, in different ways contributed to this work. First of all I would like to thank my supervisor Prof. John Ågren for supporting me, guiding me and for educational and stimulating discussions. A special thanks also for his patience with me moving from one country to another. Second, I would like to thank my assistant supervisor Dr Joakim Odquist for stimulating discussions. Dr Lars Höglund for helping me with all kinds of computer problems. Dr Walter Villanueva and Prof. Gustav Amberg for an interesting and fruitful collaboration and also for helping me with the FemLego code. Vsevolod Razumovskiy for his enthusiastic engagement in our work together. Past and present graduate students at the department of Material Science,
Finally, I would like to thank my friends and family who always support my work in the best way and Carl-Fredrik for his love and caring.

Bibliography

[1] A.W. Adamso. 1990 Physical Chemistry of Surfaces, 5th edn. New York: John Wiley & sons

[2] edited by R.M German, G.L. Messing and R.G. Cornwall. 1996 Sintering technology, New York: Marcel Dekker

[3] R.M. German. 1998 Powder Metallurgy of Iron and Steel, Ney York: John Wiley & sons

[4] R.M. German. 1985 Liquid phase sintering, Plenum Press, New York

[5] P.G. De Gennes, F. Brochard-Wyart and D. Quéré. 2004 Capillarity and Wetting Phenomena, Springer-Verlag, N.Y.,Inc

[6] W.W. Mullins. J Appl Physics, 28 (1957), 333-339

[7] W.W. Mullins. Tran Metall Soc AIME, 218 (1960), 354-361

[8] J. Crank. 1987 Free and moving boundary problems, Oxford University Press

[9] S.O. Unverdi and G. Tryggvason. J Comp Phys, 100 (1992), 25-37

[10] D. Juric and G. Tryggvason. J Comp Phys, 123 (1995), 127-148

[11] M. Sussman, P. Smereka and S. Osher. J Comp Phys, 114 (1994), 146-159

[12] S. Chen, B. Merriman, S. Osher and P. Sekerka. J Comp Phys, 135 (1997), 8-29

[13] D. Jacqmin. J Comp Phys, 155 (1999), 96-127

[14] W.J. Boettinger, J.A. Warren, C. Beckermann and A. Karma. Ann Rev Mater Res, 32 (2002), 163-194

[15] W.J. Boettinger, S.R Coriell, A.L. Greer, A. Karma, W. Kurz, M. Rapaz and R. Trivedi. Acta Mater, 48 (2000), 43-70

[16] J.W. Cahn and J.E Hilliard. J Chem Phys, 28 (1957), 258-267

[17] S.M. Allen and J.W Cahn. Acta Metall,27 (1979), 1085-1095

[18] M. Hillert. Sc.D. thesis, MIT 1956, see also: Acta Metall, 9 (1961), 525-535

[19] S-L Wang, R.F Sekerka, A.A. Wheeler, B.T. Murray, S.R Coriell, R.J. Braun and G.B. McFadden. Physica D, 69 (1993), 189-200

[20] J.A. Warren and W.J. Boettinger. Acta Mater, 43 (1995), 689-703

[21] L-Q Chen and W Wang. Physical Rev B, 50 (1994), 15752

[22] I. Steinbach, F.Pezzola, B. Nestler, M. Beebelber, R.Prieler, G.J. Schmitz and J.L.L. Rezende. Physica D, 94 (1996), 135-147

[23] D. Jacqmin. J Fluid Mech, 402 (2000), 57-88

[24] W. Villanueva and G Amberg. Int J Multiphase Flow, 32 (2006), 1072-1086

[25] L.Q. Chen. Ann Rev Mater Res, 32 (2002), 113-140

[26] J.D. van der Waals 1893: See for example English translation in: J.S. Rowlinson, Journal of statistical physics 20 (1979) 197

[27] I. Loginova, J. Ågren and G. Amberg. Acta Mater, 52 (2004), 4055-4065

[28] J.W. Cahn. Acta Metall, 9 (1961), 795-801

[29] G.S. Upadhayaya. 2000 Sintered metallic and Ceramic Materials. England: John Wiley & sons Ltd.

[30] P.G.de Gennes. Rev Mod Phys, 57 (1985), 827-863

[31] T. Young. Phil Trans R Soc Lond, 95 (1805), 65-87

[32] http://www.wikimedia.org/wik/wetting

[33] P. Shen, H. Fujii, T. Matsumoto and K. Nogi.Scr Mater, 29 (2003), 563-569

[34] L. Yin, T. Murray and T.J. Singler. Acta Mater, 54 (2006), 3561-3574

[35] R.G. Cox. J Fluid Mech, 168 (1986), 169-194

[36] R.L. Coble. J Appl Phys, 32:5 (1961), 787-792

[37] P.A. Beck. Trans AIME, 133 (1939), 222-233

[38] K. Lücke and K. Detert. Acta Metall, 5 (1957), 628-637

[39] J.W. Cahn. Acta Metall, 10 (1962), 789-798

[40] D. McLean. 1957 Grain boundaries in metals. London: Oxford University Press

[41] T. Koyama and H. Onodera. J of Phase Eq and Diff, 27:1 (2005), 22-29

[42] M. Honyu and Y. Saito. ISIJ Inter, 40:9 (2000), 914-919

[43] J. Kim and K. Kang. Appl Num Math, 59 (2009), 1029-1042

[44] A. Artemev, Y. Yin and A.G. Khachaturyan,Acta Mater, 49 (2001), 1165-1177

[45] M. Hillert and B. Sundman. Acta Metall, 24 (1976), 731-743

[46] J. Odqvist Doctoral Thesis, KTH, Stockholm, 2003

[47] J. Odqvist, B. Sundman and J. Ågren. Acta Mater, 51 (2003), 1035-1043

[48] M. Hillert. Acta Mater, 52 (2004), 5289-5293

[49] I. Loginova, J. Oqvist, G. Amberg and J. Ågren. Acta Mater, 51 (2003), 1327-1339

[50] P-R. Cha, S.G. Kim, D-H. Yeon and J-K Yoon. Acta Mater, 50 (2002), 3817-3829

[51] H. Strandlund, J. Odqvist and J. Ågren. Comp Mater Science, 44:2 (2008), 265-273

[52] J-O. Nilsson. Mater Sci Tech, 8 (1992), 685

[53] R.O. Williams and H.W. Paxton. J Iron Steel Inst, 185 (1957), 358

[54] http://www.wikimedia.org/wik/spinodal_decomposition

[55] D. Chandra and L. H. Schwartz. Metallurg Trans, 2 (1971), 511

[56] J.M. Hyde, M.K. Miller, A. Cerezo and G.D.W Smith. Appl Surf Science, 87/88 (1995), 311-317

[57] J.E. Brown and G.D.W. Smith. Surface Science 246 (1991), 285-291

[58] H.E. Exner Inter Mater Rev, 4 (1979), 149-173

[59] A. Petersson Doctoral Thesis, KTH, Stockholm, 2004

[60] W.J. Huppman and H. Riegger. Acta Mater, 23 (1975), 965

[61] G.C. Kuczynski. Trans Am Inst Min Eng, 85 (1949), 169-178

[62] R. Kieffer, H. Nowotny, A. Necker, P. Ettmayer and L. Usner, Monatshefte für Chemistry, 99 (1968), 1020-1027

[63] A. Markström and K. Frisk. CALPHAD, 33 (2009), 530-538

[64] G. Amberg, R. Tornhardt and C. Winkler. Math Comp Simulat, 49 (1999), 257-274

[65] http://www.mech.kth.se/gustava/femlego

[66] J.L. Guermond and L. Quartapelle. Proceedings of the International Conf on Finite Elements in Fluids, Venezia, October, 1995

[67] B. Sundman, B. Jansson and J-O. Andersson. Calphad, 9 (1985), 153-190

[68] J-O. Andersson, T. Helander, L. Höglund, P. Shi and B. Sundman. Calphad, 26 (2002), 273, see also http://www.thermocalc.com

[69] N. Saunders and A.P. Miodownik. (1998) CALPHAD (Calculation of the Phase Diagram): A comprehensive Guide, Pergamon

[70] J-O. Andersson and J. Ågren. J Appl Phys, 72 (1992), 1350-1355

[71] L. Höglund Sc.D. thesis, KTH, Stockholm, 1997

[72] A. Borgenstam, A. Engström. L. Höglund and J. Ågren. J Phase Eq, 21 (2000), 269-280

[73] T. Kitashima. Philosophical Mag, 88 (2008), 1615-1637

[74] http://www.micress.de

[75] S. Novy, P. Pareige and C. Pareige J of Nuclear Mater. 2009; 384: 96-102